Journal of Experimental Botany, Vol. 55, No. 402, pp. 1569–1575, July 2004
DOI: 10.1093/jxb/erh173 Advance Access publication 4 June, 2004

Journal of Experimental Botany

RESEARCH PAPER

Changes in pit membrane porosity due to deflection and stretching: the role of vestured pits

Brendan Choat[1,*], Steven Jansen[2], Maciej A. Zwieniecki[1], Erik Smets[2] and N. Michele Holbrook[1]

[1] *Department of Organismic and Evolutionary Biology, Harvard University, Cambridge, Massachusetts, MA 02138, USA*

[2] *Laboratory of Plant Systematics, K.U. Leuven, Institute of Botany and Microbiology, Kasteelpark Arenberg 31, B-3001 Leuven, Belgium*

Received 10 November 2003; Accepted 7 April 2004

Abstract

The effect of increasing pressure difference (ΔP) on intervessel pit membrane porosity was studied in two angiosperm tree species with differing pit architecture. *Fraxinus americana* L. possesses typical angiosperm bordered pit structure while *Sophora japonica* L. exhibits well-developed vestures in intervessel pit chambers. It was hypothesized (a) that large ΔP across intervessel pits would cause the deflection of pit membranes in the stems of *F. americana* resulting in significant increases in porosity and thus lower cavitation thresholds, and (b) that the presence of vestures would prevent the deflection of pit membranes in *S. japonica*. To determine if the porosity of pit membranes increased under mechanical stress, suspensions of colloidal gold, 5 nm and 20 nm in diameter, were perfused across intervessel pit membranes at ΔP ranging from 0.25 MPa to 6.0 MPa. The effect of increasing ΔP on membrane porosity was also tested by comparing air seeding thresholds (P_a) in stems perfused with water or a solution with lower surface tension. Air seeding and colloidal gold experiments indicated that pit membrane porosity increased significantly with ΔP in *F. americana*. In *S. japonica*, increases in permeability to colloidal gold with ΔP were small and maximum pore diameters predicted from P_a were independent of ΔP, suggesting that vestures limited the degree to which the membrane can be deflected from the centre of the pit cavity. This provides the first experimental evidence that vestures reduce the probability of air seeding through pit membranes.

Key words: Air seeding, cavitation, deflection, pit membranes, porosity, vestures, xylem.

Introduction

Intervessel pit membranes are modified primary cell walls consisting of tightly interwoven cellulose microfibrils in a matrix of hydrated hemicellulose and pectins (Brett and Waldron, 1996). The finely porous membranes are designed to allow the flow of water between adjacent vessels while preventing the passage of gas bubbles and pathogens. Vulnerability to water-stress-induced embolism has been related to the porosity of pit membranes by a process known as air seeding (Sperry and Tyree, 1988). When a xylem vessel containing an embolism lies adjacent to a functional vessel containing liquid under tension, a substantial pressure difference can develop across the pit membranes which connect the vessels. At a critical pressure difference that scales inversely with the size of the largest pore, gas will penetrate the pit membrane and the embolism will expand into the previously water-filled vessel (Tyree and Zimmermann, 2002).

A major challenge to understanding water-stress-induced embolism is the discrepancy between empirical measurements of pit membrane pore sizes and those calculated from measurements of air seeding pressure differences (Choat *et al.*, 2003). Electron micrographs of pit membranes often do not reveal pores in the expected size range (Schmid and Machado, 1968; Wheeler, 1983; Sano and Fukazawa, 1994; Choat *et al.*, 2003). While some studies using polystyrene microspheres have shown good correlation between membrane porosity and vulnerability to embolism (Jarbeau *et al.*, 1995), recent experiments with colloidal gold have indicated that pit membrane pores in angiosperm species were smaller than expected based on air seeding thresholds (Shane *et al.*, 2000; Choat *et al.*, 2003). Both particle perfusion experiments and electron micrographs measure

* To whom correspondence should be addressed. Fax: +1 617 496 5854. E-mail: bchoat@fas.harvard.edu

membrane pore size in a relaxed state. The possibility that deflection of intervessel pit membranes results in temporarily increased porosity has been suggested to explain the difference in pore diameters calculated from vulnerability curves and those observed using scanning electron microscopy (Hacke and Sperry, 2001; Choat *et al.*, 2003).

The degree of stretching that a pit membrane undergoes will depend upon both the dimensions and mechanical properties of the pit membrane itself as well as the geometry of the pit chamber (Tyree and Zimmermann, 2002; Sperry and Hacke, 2004). Angiosperm vessels possess bordered pits in which the secondary walls overarch the pit membrane (Dickison, 2000). Thus, the shape and dimensions of the pit chamber and the outer pit aperture provide an absolute limit to the extent to which pit membranes can deform under pressure. Some woody angiosperm species possess outgrowths from the secondary cell wall of bordered pits known as vestures (Jansen *et al.*, 1998*b*), which, when located within the pit cavity, will limit the degree to which pit membranes can be displaced. The distribution of species with vestured pits is skewed toward environments in which high transpiration rates or high xylem tensions are expected, i.e. deserts and tropical, seasonal woodlands (Jansen *et al.*, 2003; S Jansen, unpublished data), leading to the suggestion that vestures might decrease the chances of pit membrane aspiration or rupture by supporting the membrane against large pressure drops (Zweypfenning, 1978; Sperry, 2003). It has also been suggested that vestures may aid in the dissolution of emboli and in the restoration of vessels to a functional state (Carlquist, 1982, 2001; Jansen *et al.*, 2003).

In this study it was investigated how pressure influences the porosity of pit membranes in two angiosperm tree species with differing pit geometry. White ash (*Fraxinus americana* L.) has the typical bordered pit structure of angiosperm trees, but possesses minutely developed vestures on some intervessel pits, mainly in the narrow latewood vessels (Wheeler, 1981; Baas *et al.*, 1988). The pagoda tree (*Sophora japonica* L.), has bordered pits that are always distinctly vestured (Ohtani *et al.*, 1984). It was hypothesized that (i) the porosity of pit membranes could be altered by experimentally imposing a range of pressure differences (ΔP) across membranes separating two xylem vessels, and (ii) the extent to which porosity would increase with ΔP would be related to the geometry of the pit chamber and the presence of vestures.

Materials and methods

Changes in pit membrane porosity

Branches were collected from *F. americana* and *S. japonica* during the growing season of 2003 from mature trees growing at the Arnold Arboretum or on the main campus of Harvard University. The porosity of pit membranes between two adjacent vessels was measured using the microcapillary technique described in Zwieniecki *et al.* (2001). An outline of the experimental procedure used is shown in Fig. 1. Two-year-old stem segments 3–8 cm in length were cut from lateral branches, trimmed with a razor blade at each end, and flushed with filtered (0.22 μm) deionized water. Three or four replicate stem segments were tested for each species. Glass microcapillaries were pulled on a pipette puller (Pul1, World Precision Instruments, Sarasota, FL) and their tips were subsequently broken such that the opening of the capillary was in the same range as vessel diameters of the species used (50–150 μm). The capillary tip was inserted into a vessel lumen in the most recent year's growth using a ×50 stereo microscope (SZ-STB2, Olympus, Tokyo) and glued in place using cyanoacrylic glue (Loctite superbond, 409). Air was then pushed through the vessel at low pressure (≈0.1 MPa) to determine if the vessel was continuous through the segment. Segments with

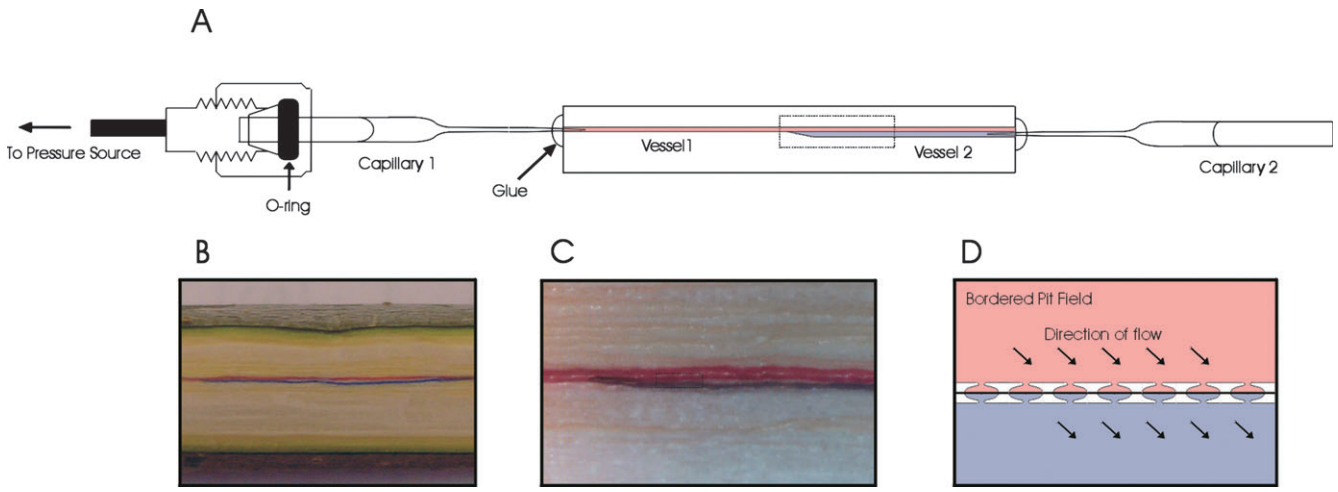

Fig. 1. Experimental protocol used to determine changes in membrane porosity (A). A microcapillary is inserted into an open vessel and sealed using cyanoacrylic glue. The vessel is stained with safranin for identification at the distal end of the stem. A second microcapillary is inserted into a vessel directly connected to the first vessel. The capillary and stem are connected to a pressure source by a compression fitting and the gold colloid suspension is perfused through the stem. Exudate samples are collected from the distal capillary. When perfusion experiments are completed the second vessel is stained with toluidine blue. The stem segments were then sectioned longitudinally to expose the vessels and check that a direct connection existed between the vessels (B, C). This ensured that perfusate passed across a single bordered pit membranes (D).

blocked vessels or ones in which the vessel ended within the segment were discarded. The vessel was stained with 0.01% safranin for identification at the distal end of the segment and then trimmed back with a razor blade at the distal end until a direct connection was observed between the stained vessel and a second vessel. The lumen of the original (stained) vessel was then carefully blocked with glue at the distal end of the segment and a capillary was inserted into the adjacent vessel. This procedure ensured that the perfusing solution only passed through one bordered pit field. The stem segment was then connected to a pressure source by attachment of a compression fitting to the proximal microcapillary and the two vessels were flushed with filtered, deionized water at 2.0 MPa to remove excess stain or residual gas pockets.

The porosity of intervessel pit membranes was quantified by perfusing the samples with suspensions of colloidal gold containing either 5 nm or 20 nm particles (100 μl l^{-1} as $HAuCl_4$; Sigma Aldrich, St Louis). Samples were first perfused at a pressure of 2.0 MPa. The procedure was then repeated at 4.0 MPa and 6.0 MPa. After this, the samples were perfused at lower pressures of 1.0, 0.5, and 0.25 MPa. Between each perfusion the distal microcapillary was flushed with deionized water. Droplets of exudate (2.5 μl volume) collected at each delivery pressure were dried at ambient temperature on carbon discs. Samples of undiluted suspension were also dried onto carbon discs. Each sample was tested for the presence of gold using energy dispersive X-ray analysis (EDX) in a scanning electron microscope (FEI Quanta 200, Hillsboro, Oregon). Observations were performed through a soft X-ray window at 30 kV and ×10 000 magnification. Three measurements were made for each sample droplet.

After exudate samples had been collected at each delivery pressure, the segments were removed from the injection apparatus and the second vessel was stained with toluidine blue (0.01%) from the distal (downstream) end. The stem segment was then sectioned longitudinally to check that there was a direct connection between the two vessels. Preliminary experiments to test whether pit membranes ruptured when exposed to high pressures were conducted using a sequential increase and decrease of perfusion pressures (0.25, 0.5, 1.0, 2.0, 4.0, 6.0, and 0.25 MPa). In no instance was there an increase in the amount of gold in the exudate following the second low-pressure (0.25 MPa) perfusion, indicating that 6.0 MPa did not result in irreversible changes in membrane permeability.

Air seeding threshold

The air seeding threshold (P_a) for intervessel pit membranes was measured in individual vessels for each species (Melcher *et al.*, 2003). To investigate how pit membrane deflection and stretching may affect membrane porosity, liquids of different surface tension (τ) were used to alter the P_a of each species. The two liquids used were deionized water (τ=0.072 N m^{-1}) and 0.1% (w/v) Triton X (τ=0.031 N m^{-1}). Branches were collected from the same trees used in the gold perfusion experiments and seven to nine replicate stem segments were tested for each treatment. In the laboratory, short segments (length 4–8 cm) were cut from the branches, shaved at each end with a razor blade, and flushed with either deionized water or Triton X. Microcapillaries were glued into two connected vessels as described above. The proximal capillary was filled with either water or Triton×and connected to the pressure source by a compression fitting. Nitrogen gas was delivered at a pressure of 0.1–0.5 MPa to the proximal capillary. After all of the liquid from the proximal capillary had moved into the distal capillary the system was left for 60 s at a pressure of 0.5 MPa. If no bubbles appeared in the distal capillary, it was assumed that an intact pit field existed between the capillaries. The pressure was then increased in 0.05 MPa steps at 30 s intervals until gas appeared in the distal capillary. This was taken as the threshold pressure for gas penetration of the intervessel pit membranes between the two vessels. Maximum pit membrane pore diameters were calculated from air seeding thresholds for each species using

$$D = \frac{4\tau\cos\theta}{\Delta P} \quad (1)$$

where ΔP is the pressure difference across the membrane, τ is the surface tension of the fluid, θ is the contact angle between the air water interface and the pit membrane (assumed to be 0), and D is the diameter of the pore.

Anatomy

Longitudinal and transverse sections were cut with a sliding microtome and observed using scanning electron (SEM) and light microscopy (LM) to determine the geometry of pits for each of the species (Jansen *et al.*, 1998*a*). Measurements of pit membrane radius (r) and depth of pit chamber (d) were made on LM and SEM images using Carnoy 2.0 software (Schols *et al.*, 2002). The depth of the pit chamber was defined as the distance from the pit membrane to the outer aperture of the pit chamber.

The maximum expansion (stretching) of pit membranes was estimated assuming that the membrane deflection would be limited by the depth (d) of the pit chamber in each species (Fig. 2). It was assumed that the membrane expands to form a segment of a sphere. The increase in surface area (ΔA_{max}) was calculated as the expansion of a flat membrane of radius r to a segment of a sphere from:

$$\Delta A_{max} = \frac{2\pi R d}{2\pi r} \quad (2)$$

where R is the radius of the sphere inscribed by the expanded membrane (Gieck and Gieck, 1997). Although the inflation of uniform circular diaphragms composed of isotropic materials does not strictly expand into a segment of a sphere (Adkins and Rivlin, 1952), the effect on ΔA_{max} is small.

Results

Gold penetration of pit membranes

The amount of gold penetrating between vessels increased with pressure for both 5 nm and 20 nm colloidal particles in both species, however, the increase was much greater in *F. americana* than in *S. japonica* (Fig. 3). The small increase in gold penetration observed for *S. japonica* was not significantly different (P>0.05; Tukey HSD, two-way ANOVA; n=3–4) with 5 nm or 20 nm gold. The amount of 5 nm gold was greater in samples from *F. americana* than in *S. japonica* at delivery pressures above 0.5 MPa; particles of this diameter penetrated pit membranes of *F. americana* to some degree even at the lowest delivery pressures (0.25 MPa). In both species, very little 20 nm gold penetrated below a 2.0 MPa delivery pressure. At 2.0 MPa, there was a significant increase in the amount of 20 nm particles penetrating membranes of *F. americana*. Measurements of suspensions supplied to the test segments demonstrated that some proportion of colloidal particles was filtered by pit membranes even at high delivery pressures.

Air seeding pressures

Air seeding thresholds (P_a) obtained using deionized water were higher for *S. japonica* (2.62±0.18 MPa) than for

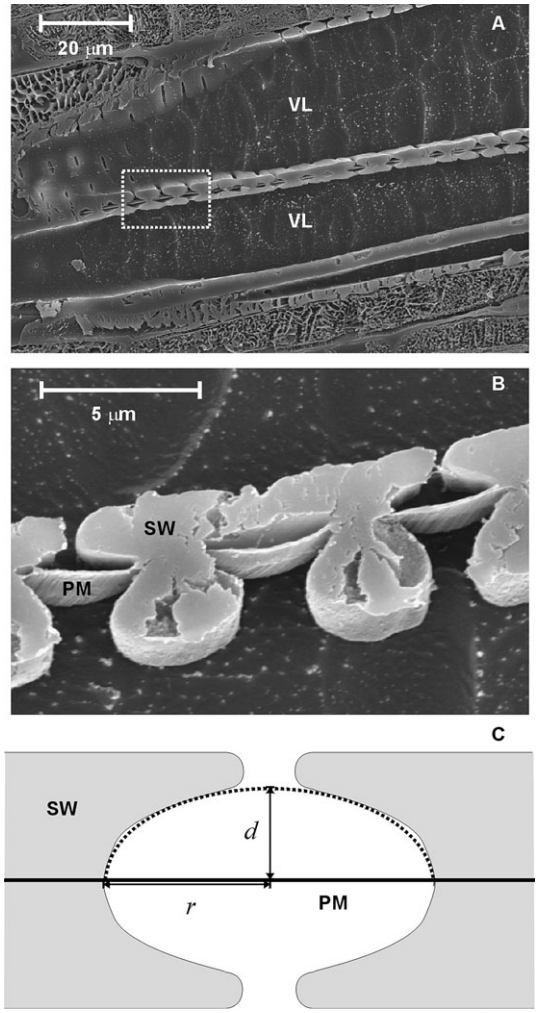

Fig. 2. Bordered pit structure in angiosperms. (A) Cryo-electron micrograph showing a longitudinal section with two xylem vessels connected by a bordered field; VL, vessel lumen. (B) Closer detail of bordered pits (from dashed box in (A)) with overarching secondary walls (SW) and pit membranes (PM). (C) Diagram of bordered pit showing resting (solid line) and stretched (dashed line) positions of pit membrane (PM) with initial radius (*r*) and depth of the pit chamber (*d*).

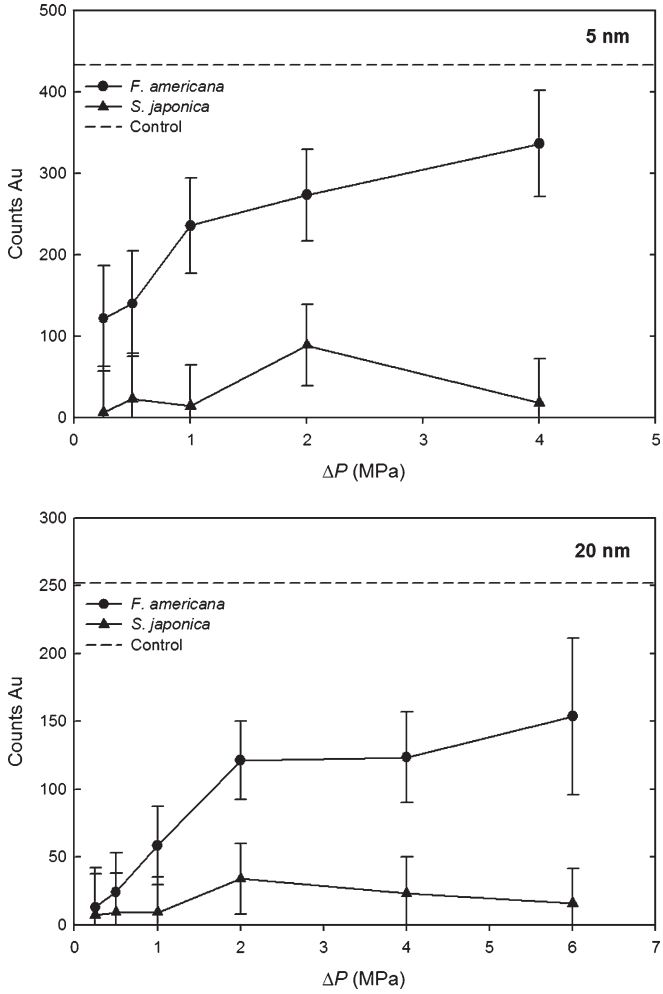

Fig. 3. Amount of colloidal gold penetrating intervessel pit membranes with increasing pressure difference (ΔP) in *Fraxinus americana* and *Sophora japonica*. The amount of gold penetration (Counts Au) was determined by energy dispersive X-ray analysis for 5 nm gold colloids and 20 nm colloids. Counts of gold were determined from analysis of 2.5 μl samples dried onto carbon tape. Values for unfiltered suspensions of colloidal gold are shown as dashed lines. Note the difference in scales in the *x* and *y* axes between the 5 nm and 20 nm plots. Error bars show 95% confidence intervals (two-way ANOVA).

F. americana (1.92±0.10 MPa), however, P_a was similar for stems perfused with Triton X (Table 1). The mean (±SE) pit membrane pore diameter calculated for *F. americana* stems perfused with deionized water (152±8 nm; n=7) was significantly wider (P<0.05; t-test) than the mean pore diameter calculated for stems perfused with Triton X (117±13 nm; n=9). By contrast, for *S. japonica* mean pore diameter was not significantly different (P=0.93; t-test) between deionized water (114±8 nm; n=8) and Triton X (115±10 nm; n=7) treatments. Thus, while pore size increased at higher ΔP for *F. americana*, there was no change in estimated pore size for *S. japonica* between 1.13 MPa and 2.62 MPa.

Anatomy

F. americana had smaller pits, with a mean membrane radius of 1.95 μm compared with 2.71 μm for *S. japonica* (Table 2). *F. americana* also had a smaller pit chamber depth (0.61 μm) than *S. japonica* (0.84 μm). The vestures in *S. japonica* vary from small and unbranched to largely branched and widely expanding (Fig. 4). Minutely vestured pits occur in *F. americana*, especially in the narrow latewood vessels, while intervessel pits of the wide, earlywood vessels have non-vestured pits.

The calculated maximum pit membrane stretch differed between the species based on the ratio of the depth of the pit chamber to the radius of the pit membrane (d:r). Despite the difference in pit size, the d:r ratio was similar for the two species (0.31) if vestures were not considered (Table 2). However, the presence of vestures results in the effective depth of the pit chamber being very small (≈0.2 μm), allowing for little deflection to occur. Thus the maximum

Table 1. *Air seeding threshold (P_a) and estimated pit membrane pore diameter (D) for two angiosperm tree species perfused with liquids of different surface tension (τ): water (τ=0.072 N m^{-1}) and 0.1% (w/v) Triton X (τ=0.031 N m^{-1})*

Membrane pore diameters were calculated from equation 1. Note that each pore diameter is a mean of calculated diameters rather than a diameter calculated from the mean value of P_a. Standard errors are given in parentheses (n=7–9). Within each row, different letters represent a significant difference (P<0.05; t-test) in calculated pore diameter.

Species	Water		Triton X	
	P_a (MPa)	D (nm)	P_a (MPa)	D (nm)
Fraxinus americana	1.93 (±0.10)	152 (±8) a	1.17 (±0.10)	117 (±13) b
Sophora japonica	2.62 (±0.18)	114 (±8) a	1.13 (±0.10)	115 (±10) a

Table 2. *Anatomical characteristics of intervessel pits for two angiosperm tree species*

Radius of pit membrane (r), depth of pit chamber (d), and ratio of pit chamber depth to pit membrane radius (d:r). Data are given for *S. japonica* with vestures (wv) and without (wov). The increase in surface area of stretched membranes as a proportion of the initial membrane area (ΔA_{max}) was calculated from equation 2 using values of d and r listed for each species. Values of r and d are means of 50 and 20 measurements, respectively, with SE in parentheses.

Species	r (μm)	d (μm)	d:r	ΔA_{max} (%)
Fraxinus americana	1.95 (±0.08)	0.61 (±0.07)	0.31	8.9
Sophora japonica (wov)	2.71 (±0.09)	0.84 (±0.04)	0.31	8.8
Sophora japonica (wv)	2.71 (±0.09)	0.20 (±0.01)	0.07	0.5

increase in surface area as a proportion of the initial pit membrane surface area (ΔA_{max}) is expected to be larger in *F. americana* (8.9%) than in *S. japonica* (0.5%). In addition, it is possible that a greater increase in surface area may occur if the pit membrane stretches through the aperture of the pit chamber in *F. americana*. It is assumed that vestures would prevent this occurring is *S. japonica*.

Discussion

The principal aim of this study was to determine whether the deformation of intervessel pit membranes plays a significant role in determining the vulnerability of a species to water-stress-induced cavitation. If this is the case then it could (i) explain the difficultly in observing pores in the size range predicted from vulnerability curves and (ii) provide support for the hypothesis that vestures reduce the vulnerability of a species to cavitation by preventing deflection of the membrane.

Data from experiments with colloidal gold indicated that increases in pit membrane porosity with ΔP were greater for *F. americana* than for *S. japonica*. This is consistent with the occurrence of stretching in membranes of *F. americana* and the hypothesis that vestures may limit stretching and deflection of the pit membrane in *S. japonica*. However, the influence of this increase in porosity on air seeding is complicated by the fact that pore sizes calculated for air seeding for both species were 5–10 times greater than the size of colloidal gold particles used to estimate porosity. Experiments using surfactant to alter the pressure difference at which P_a occurred provided no evidence of an increase in pore diameter caused by stretching in *S. japonica*; estimated pore diameter for *F. americana* increased significantly between ΔP of 1.17 MPa and 1.93 MPa. It is proposed that the increase in porosity with ΔP observed in *F. americana* was a result of deflection and stretching of the pit membranes.

There was some disparity between data collected from gas penetration and gold perfusion experiments. For instance, penetration of 5 nm gold particles through the pit membranes of *S. japonica* increased with ΔP (Fig. 3), but this increase was not apparent in air seeding experiments. This disparity is likely to relate to the different ways in which these methods estimate membrane pore size. Because air seeding will always occur first at the largest pore, the values obtained from gas penetration experiments represent the diameters of the largest wetted pores in the membranes (Tyree and Zimmermann, 2002). Assuming that there is a normal distribution of pore diameters within a population of pit membranes that connects two vessels, it is only the very tail of this distribution that would be responsible for air seeding events. Membrane porosity measured with colloidal gold should be more sensitive to the mean pore size, as the amount of gold allowed through the membrane by a small number of large pores is likely to be below the limits of detection by EDX.

From the few studies that have examined the structure of angiosperm intervessel pit membranes in detail, it appears that the membranes consist of a number of distinct layers of microfibrils on either side of the middle lamella (Schmid, 1965; Schmid and Machado, 1968). The layers of microfibrils have different orientations, with layers formed prior to cell expansion having a primarily parallel orientation, while those formed after cell expansion exhibit a random orientation. Based on this arrangement of cell wall components, it is apparent that most pathways through the membrane would be complex and tortuous rather than straight channels. Electron micrographs also suggest that the majority of pit membranes pores have an effective diameter of 5–20 nm, close to that of primary cell walls

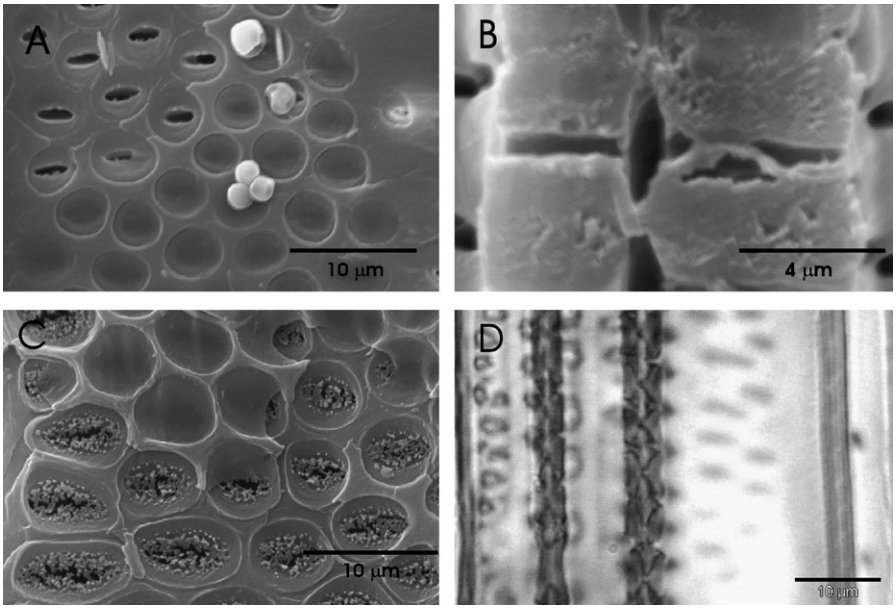

Fig. 4. Light and scanning electron micrographs of pit structure in (A, B) *Fraxinus americana* and (C, D) *Sophora japonica*. Well-developed vestures are visible in the pit chamber of *S. japonica.*

from living cells (Wheeler, 1981, 1983; Choat *et al.*, 2003). While the experimental data presented here support the interpretation that there is a temporary increase in the porosity of pit membranes with increasing ΔP, they do not indicate that a small (5–20 nm) pore would expand to a 100–150 nm pore across the range of pressures at which air seeding occurred. It is likely that the large pores responsible for air seeding would be visible, even in a relaxed state, at the resolutions obtainable with an SEM, i.e. 50–100 nm in diameter. Therefore, the most likely explanation for the difficulty in direct observation of large pores is that they are rare enough to avoid detection and occur in only a few of the thousands of pit membranes which connect two vessels.

An increase in porosity was not observed in the pit membranes of *S. japonica* by either experimental method used. Thus, the data presented here provide the first experimental evidence that vestures reduce the vulnerability of plants to water-stress-induced cavitation, a function long postulated by wood anatomists concerned with ecological aspects of xylem anatomy (Zweypfenning, 1978; Carlquist, 1982; Jansen *et al.*, 2003). However, confirmation of this hypothesis will require further experimentation involving a greater sample size of species with vestured and non-vestured pits. It is also clear that other factors, relating to the size and frequency of larger pores, are equally if not more important than the potential for deflection and stretching of pit membranes in determining the underlying vulnerability to cavitation of a species. This is highlighted by the fact that the presence of vestures is not an essential trait for drought tolerance, and many species existing in arid regions lack vestures but maintain high cavitation thresholds (Jansen *et al.*, 1998*b*). Finally, it is presumed that some cost will accompany the benefits bestowed by vestures, most likely in the form of increased resistance to flow through the bordered pit chamber. Further study is required to determine the constraints that such structures may place on water transport.

Acknowledgements

We thank Richard Schalek for assistance with electron microscopy and EDX analysis. This research was supported by grants from the Andrew W Mellon Foundation, the USDA (NRICGP 2001-35100-10615), and the National Science Foundation (IBN 0078155). Steven Jansen is a postdoctoral fellow of the Fund for Scientific Research, Flanders (Belgium) (FWO, Vlaanderen) and his visit to Harvard University was supported by a grant from the FWO, Vlaanderen.

References

Adkins JE, Rivlin RS. 1952. Large elastic deformations of isotropic materials. IX. The deformation of thin shells. *Philosophical Transactions of the Royal Society of London, Series A, Mathematical and Physical Sciences* **244,** 505–531.

Baas P, Esser PM, Vanderwesten MET, Zandee M. 1988. Wood anatomy of the Oleaceae. *International Association of Wood Anatomists Bulletin* **9,** 103–182.

Brett C, Waldron K. 1996. Physiology and biochemistry of plant cell walls. In: Black M, Charlwood B, eds. *Topics in plant functional biology*. London, Chapman & Hall.

Carlquist S. 1982. Wood anatomy of Onagraceae: further species; root anatomy; significance of vestured pits and allied structures in dicotyledons. *Annals of the Missouri Botanical Garden* **69,** 755–769.

Carlquist S. 2001. C*omparative wood anatomy. Systematic, ecological, and evolutionary aspects of dicotelydon wood*. Berlin: Springer-Verlag.

Choat B, Ball M, Luly J, Holtum J. 2003. Pit membrane porosity and water stress-induced cavitation in four co-existing dry rainforest tree species. *Plant Physiology* **131,** 41–48.

Dickison WC. 2000. *Integrative plant anatomy*. New York: Academic Press.

Gieck K, Gieck R. 1997. *Engineering formulas,* 7th edn. New York: McGraw-Hill Professional.

Hacke UG, Sperry JS. 2001. Functional and ecological xylem anatomy. *Perspectives in Plant Ecology, Evolution and Systematics* **4,** 97–115.

Jansen S, Baas P, Gasson P, Smets E. 2003. Vestured pits: do they promote safer water transport? *International Journal of Plant Sciences* **164,** 405–413.

Jansen S, Kitin P, de Pauw H, Idris M, Beeckman H, Smets E. 1998*a*. Preparation of wood specimens for transmitted light microscopy and scanning electron microscopy. *Belgian Journal of Botany* **131,** 41–49.

Jansen S, Smets E, Baas P. 1998*b*. Vestures in woody plants: a review. *International Association of Wood Anatomists Journal* **19,** 347–382.

Jarbeau JA, Ewers FW, Davis SD. 1995. The mechanism of water-stress-induced embolism in two species of chaparral shrubs. *Plant, Cell and Environment* **18,** 189–196.

Melcher PJ, Zwieniecki MA, Holbrook NM. 2003. Vulnerability of xylem vessels to cavitation in sugar maple. Scaling from individual vessels to whole branches. *Plant Physiology* **131,** 1775–1780.

Ohtani J, Meylan BA, Butterfield BG. 1984. Vestures or warts—proposed terminology. *International Association of Wood Anatomists Bulletin* **5,** 3–8.

Sano Y, Fukuzawa K. 1994. Structural variations and secondary changes in pit membranes in *Fraxinus mandshurica* var. *japonica*. *International Association of Wood Anatomists Journal* **15,** 283–291.

Schmid R. 1965. Fine pits in hardwoods. In: Cote WA, ed. *Cellular ultrastrcture of woody plants*. New York: Syracuse University Press, 291–304.

Schmid R, Machado RD. 1968. Pit membranes in hardwoods—fine structure and development. *Protoplasma* **66,** 185–204.

Schols P, Dessein S, D'Hondt C, Huysmans S, Smets E. 2002. Carnoy: a new digital measurement tool for palynology. *Grana* **41,** 124–126.

Shane MW, McCully ME, Canny MJ. 2000. Architecture of branch–root junctions in maize: structure of the connecting xylem and the porosity of pit membranes. *Annals of Botany* **85,** 613–624.

Sperry JS. 2003. Evolution of water transport and xylem structure. *International Journal of Plant Sciences* **164,** S115–S127.

Sperry JS, Hacke UG. 2004. Analysis of circular bordered pit function. I. Angiosperm vessels with homogenous pit membranes. *American Journal of Botany* **91,** 369–385.

Sperry JS, Tyree MT. 1988. Mechanism of water stress-induced xylem embolism. *Plant Physiology* **88,** 581–587.

Tyree MT, Zimmermann MH. 2002. *Xylem structure and the ascent of sap*. New York: Springer-Verlag.

Wheeler EA. 1981. Intervascular pitting in *Fraxinus americana* L. *International Association of Wood Anatomists Bulletin* **2,** 169–174.

Wheeler EA. 1983. Intervascular pit membranes in *Ulmus* and *Celtis* native to the United States. *International Association of Wood Anatomists Bulletin* **4,** 79–88.

Zweypfenning RCVJ. 1978. A hypothesis on the function of vestured pits. *International Association of Wood Anatomists Bulletin* **1,** 13–15.

Zwieniecki MA, Melcher PJ, Holbrook NM. 2001. Hydraulic properties of individual xylem vessels of *Fraxinus americana*. *Journal of Experimental Botany* **52,** 257–264.